





Peat humification- and $\delta^{13}\text{C}_{\text{cellulose}}$ -recorded warm-season moisture variations during the past 500 years in the southern Altai Mountains within northern Xinjiang of China

ZHANG Dong-liang^{1,2*}  <http://orcid.org/0000-0001-6655-096X>;  e-mail: zhdxieg@163.com

YANG Yun-peng^{1,2}  <http://orcid.org/0000-0002-1506-8265>; e-mail: yangyunpeng15@mails.ucas.edu.cn

LAN Bo³  <http://orcid.org/0000-0002-6685-539X>; e-mail: boblan2004@163.com

* Corresponding author

¹ Xinjiang Institute of Ecology and Geography, Chinese Academy of Sciences, Urumqi 830011, China

² University of Chinese Academy of Sciences, Beijing 100049, China

³ School of Environmental and Chemical Engineering, Chongqing Three Gorges University, Chongqing 404000, China

Citation: Zhang DL, Yang YP, Lan B (2017) Peat humification- and $\delta^{13}\text{C}_{\text{cellulose}}$ -recorded warm-season moisture variations during the past 500 years in the southern Altai Mountains within northern Xinjiang of China. *Journal of Mountain Science* 14(11). <https://doi.org/10.1007/s11629-017-4538-1>

© Science Press and Institute of Mountain Hazards and Environment, CAS and Springer-Verlag GmbH Germany 2017

Abstract: To predict future spatio-temporal patterns of climate change, we should fully understand the spatio-temporal patterns of climate change during the past millennium. But, we are not yet able to delineate the patterns because the qualities of the retrieved proxy records and the spatial coverage of those records are not adequate. Northern Xinjiang of China is one of such areas where the records are not adequate. Here, we present a 500-yr land-surface moisture sequence from Heiyangpo Peat (48.34°N, 87.18°E, 1353 m a.s.l) in the southern Altai Mountains within northern Xinjiang. Specifically, peat carbon isotope value of cellulose ($\delta^{13}\text{C}_{\text{cellulose}}$) was used to estimate the warm-season moisture variations and the degree of humification was used to constrain the $\delta^{13}\text{C}_{\text{cellulose}}$ -based hydrological interpretation. The climatic attributions of the interpreted hydrological variations were based on the warm-season temperature reconstructed from Belukha ice core and the warm-season precipitation inferred from the reconstructed Atlantic Multidecadal Oscillations (AMO). The results show that humification decreased and the $\delta^{13}\text{C}_{\text{cellulose}}$ -suggested moisture decreased from ~1510 to ~1775 AD, implying that a constant drying

condition may have inhibited peat decay. Our comparison with reconstructed climatic parameters suggests that the moisture-level decline was most likely resulted from a constant decline of precipitation. The results also show that humification kept a stable level and the $\delta^{13}\text{C}_{\text{cellulose}}$ -suggested moisture also decreased from ~1775 to ~2013 AD, implying that peat decay in the acrotelm primarily did not depend on the water availability or an aerobic environment. Again, our comparison with reconstructed climatic parameters suggests that the land-surface moisture-level decline was most likely resulted from a steady warming of growing-season temperature.

Keywords: Peat; Carbon isotope of cellulose; Humification; Warm-season moisture; Southern Altai Mountains

Introduction

The earth's surface has undergone a significant warming at an unprecedented pace in the past century (IPCC 2014) and the fastest warming occurred in northern mid-latitudes zones (Batima

Received: 31 May 2017
Revised: 18 August 2017
Accepted: 27 September 2017

et al. 2005; Fei et al. 2014; Salnikov et al. 2015; Xu et al. 2010). The warming is reported to have reduced the effective soil moisture and expanded the areal extent of drylands via an enhancement of evaporation (Huang et al. 2015), thus directly threatening the ecological security and the economic sustainability of these drylands (IPCC 2014). Northern Xinjiang, where our study area (i.e., the southern Altai Mountains) is situated, belongs to the aforementioned fastest-warming northern mid-latitudes and also is in the middle of the central-Asian drylands (Figure 1). Unlike many other drylands where the annual precipitation has been declining, the annual precipitation in northern Xinjiang and also in the immediate adjacent areas has been increasing during the instrument-recording period (i.e., past ~60 years) with the warm-season increase being the least significant (Xu et al. 2015).

The effect of the large-scale warming is a considerable decline in the effective soil moisture during the growing season in northern Xinjiang and also in the immediate adjacent areas despite of the observed increase in the annual precipitation (Xu et al. 2015). It simply means that the future ecological security will be threatened by an extensive reduction in net primary productivity under the projected future warming. Nevertheless, the threat to water resource-related economic

sustainability will not be imminent until the turning point of glacier melting-related runoff generation is reached (Chen et al. 2012; Sorg et al. 2012). The turning point refers to the runoff transition from an increasing trend to a decreasing trend within glacier melt-water supplying watersheds under a warming climate. The runoff decrease after the turning point will pose a great threat to the economic sustainability in northern Xinjiang and also in the immediate adjacent areas under the projected future warming.

To unveil the importance of other relevant factors, we need to establish longer-term spatio-temporal patterns of past climate change. For example, to predict future spatio-temporal patterns of climate change, we should at least fully understand the spatio-temporal patterns of climate change during the past millennium (IPCC 2014; Mann et al. 2009). But, the reality is that we are not yet able to delineate the patterns because the qualities of the retrieved proxy records and the spatial coverage of those records (especially moisture records) are not adequate. The well-dated peat was received due attention for providing abundant paleomosture records (e.g., humification and cellulose carbon isotope). The humification was widely used as a proxy for the degree of peat decomposition (Castro et al. 2015; Huang et al. 2013) and cellulose carbon isotope was used as a

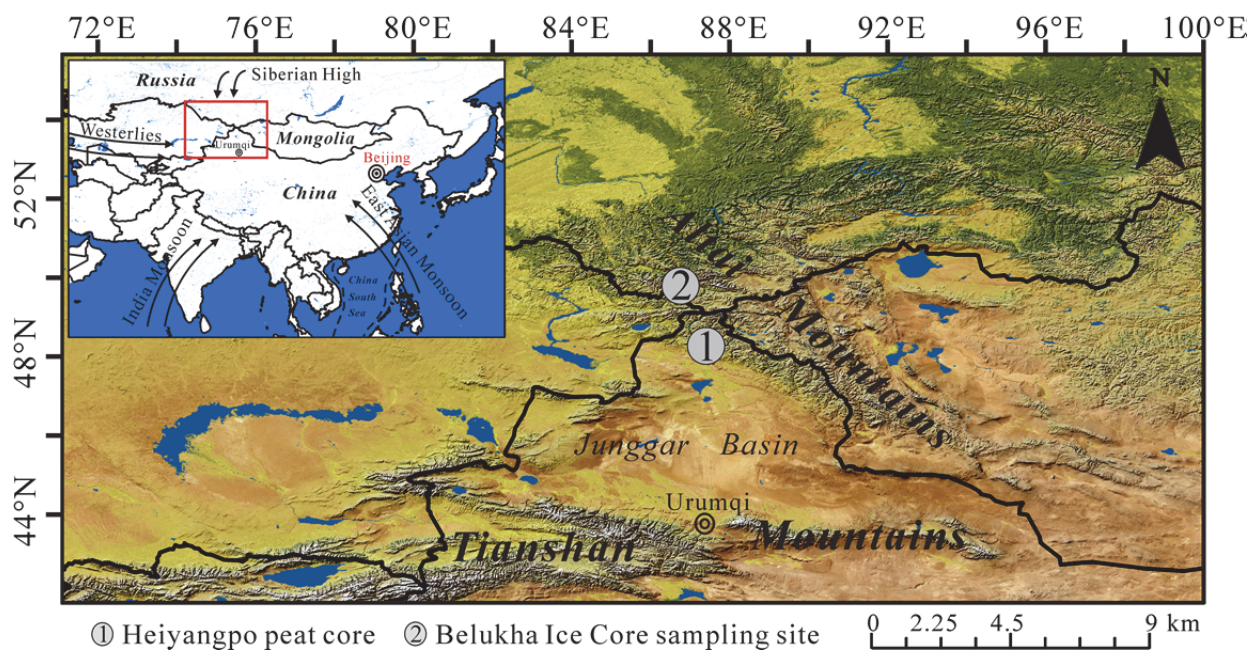


Figure 1 Geographic contexts of Heiyangpo Peat (HYP) and the referred Belukha Ice Core.

proxy for warm-season moisture (Hong et al. 2001, 2005, 2014) in palaeoclimatic and palaeohydrological reconstructions. This research reconstructed the warm-season moisture variations of the past 500 years at Heiyangpo Peat (HYP) in the southern Altai Mountains within northern Xinjiang of China through analysis of peat humification and carbon isotope of cellulose ($\delta^{13}\text{C}_{\text{cellulose}}$) with an attempt to improve our understanding of the atmospheric dynamics controlling regional warm-season climate in northern Xinjiang and the immediate adjacent areas.

1 Study Area

Our study site, Heiyangpo Peat (HYP: 48.34°N, 87.18°E, 1353 m a.s.l.), is situated in the southern margin of the Altai Mountains and immediately adjacent to the Junggar Basin within northern Xinjiang of China (Figure 1). According to meteorological data, the westerly airflow prevails over the Altai Mountains and the Junggar Basin throughout the year (Aizen et al. 2006). The Siberian high-pressure system is of a great significance during winters, while the Asian low-pressure system is of a great significance during summers (Chen 2010). The Indian Ocean is reportedly able to influence the Altai and the Junggar via injecting water vapor to the Caspian Basin, which is a water vapor source to the Altai and the Junggar, either through the Indian summer monsoon or through the El Niño-Southern Oscillation (Kutzbach et al. 2013; Marriott 2007). The Pacific Ocean is also reportedly able to supply water vapor to the Altai and the Junggar either through the East Asian summer monsoon or through the El Niño-Southern Oscillation (Sun et al. 2015; Wei and Chen 2002).

The climate in northern Xinjiang including the southern Altai Mountains and the Junggar Basin is continental with fairly large annual and diurnal ranges of temperature variations. The vertical climatic differentiation from the Junggar Basin to the southern Altai Mountains is well expressed. For instance, the mean annual temperature (MAT) is above 6°C and the mean annual precipitation (MAP) is below 100 mm at 200-m elevation in the center of the Junggar Basin, while MAT is below -

15°C and MAP is above 800 mm at 4000-m elevation in the southern Altai Mountains (Chen 2010). The vegetation reflects the vertical climatic differentiation and includes taiga forests in the southern Altai, steppe-forests in the transition between the Altai and the Junggar, steppes and desert steppes at the foothills of the mountains and deserts within the basin. Heiyangpo (HYP) Peat was most likely formed by glacial moraine damming at the headwater of the Heiyangpo River during the last deglacial and is presently a sedge-dominated minerotrophic peat (Nurbayev et al. 2008). According to field surveys, the modern water-table depth of HYP Peat is less than 0.5 m and the peat is primarily fed by precipitation and by snow-melting water. HYP Peat has depths ranging from 50 to 70 cm and is dominated by such plants as *Carex*. In addition, the peat-occupied valley is surrounded by coniferous forests at higher elevations and in shady slopes (i.e., north- and northwest-facing slopes) and by steppes at lower elevations and in sunny slopes (i.e., south- and southeast-facing slopes).

2 Sampling and Laboratory Analyses

A 68-cm-long peat core was obtained from HYP using a Holland-made peat corer in 2013. The core was sliced at 2-cm intervals and sealed into plastic bags in the field for laboratory analyses. The plant macrofossils identification shows that sedges dominate the whole peat core. Stable carbon isotopes, humification and loss on ignition (LOI) were performed in the laboratories at Xinjiang Institute of Ecology and Geography, Chinese Academy of Sciences.

2.1 ^{14}C dating

Four peat sedge samples were selected and pre-treated by acid-alkali to remove carbonates and humic acid in the laboratory. The pre-treated samples were radiocarbon dated using accelerator mass spectrometry (AMS) at NSF-AMS Facility, University of Arizona (Table 1). The chronological age was calibrated to calendar years before present (BP = before 1950 AD) using IntCal13 calibration curve and 2σ probability with CALIB-6.1 programmer (Reimer et al. 2013). The age-depth

Table 1 Accelerator mass spectrometry ¹⁴C dating results of Heiyangpo Peat (HYP)

LAB code	Depth (cm)	Materials	δ ¹³ C (‰)	¹⁴ C age (yr BP)	Calibrated age (2σ)
AA104610	8	Sedge	-29.4	Post-bomb	-
AA104611	24	Sedge	-28.1	94±31	1805-1930 AD
AA104612	38	Sedge	-29.1	151±30	1718-1783 AD
AA104613	54	Sedge	-29.5	332±35	1470-1643 AD

model was then established by fitting a smooth spline curve using the “CLAM” program (Blaauw 2010) developed under the mathematics software “R” version 3.4.1 (R Development Core Team 2013).

2.2 Loss on ignition (LOI) analysis

The peat samples (about 2g) were dried at 65°C for 24h in the electric thermostatic drying oven. And then the dried samples were incinerated in muffle at 550°C for 2h and the percentages of LOI were derived via the mass loss of peat between pre-combustion and post-combustion.

2.3 Humification analysis

Humification measurements were conducted using the commonly-used alkali-extraction method (Blackford and Chambers 1993). First, dried peat samples (0.1 g) were dissolved in 50 mL of 8% NaOH and simmered for one hour. Second, the simmered samples were filtered to get a solution after cooling and then deionized water was added to the solution to reach a final volume of 100 mL. The light absorbance measurement was done at a light wavelength of 540 nm using an Agilent Technologies Cary 60 UV-Vis spectrophotometer after the 100-mL solution was further mixed for three hours. To ensure the precision and the consistency of the measurements, the solution was measured three times. The measured humification was expressed as the percentage of light transmission, which is inversely proportional to the amount of dissolved humic matter or the degree of humification (Aaby and Tauber 1975). That is, a lower percentage of light transmission denotes a higher degree of humification and a higher percentage a lower degree of humification. To eliminate the dilution effect of mineral matter in the samples, we calculated the corrected transmission via the formula of Payne and Blackford (2008). The formula is $Hc=Hr/(1/LOI)$,

where Hc is the corrected light transmission, Hr is the raw light transmission and LOI is loss on ignition expressed as a proportion. Low Hc values denote high humification, and high Hc values mean low humification.

2.4 Stable carbon isotope analysis

For stable carbon isotope analysis, peat samples were boiled with 5% NaOH and sieved with mesh diameter of 125 μm after repeatedly washing with deionized water. The residual fractions larger than 125 μm in length were manually picked under an anatomical lens (×40) and more than 200 residual fractions were prepared to extract α-cellulose. The extraction of α-cellulose was completed by following the chemical method originally described by Green (1963) and later modified by Hong et al. (2001) and Huang et al. (2015). Specifically, the manually-picked fractions were oxidized to lignin with 0.5 g sodium chlorite (NaClO₂) and 0.5 mL glacial acetic acid dissolved in 5 mL deionized water for 60 min in a water bath at 80°C. The step was repeated five times to completely get rid of lignin. The lignin-free sample was submerged into sodium hydroxide (NaOH 10%) and heated for 60 min at 80°C to hydrolyze hemicelluloses to yield α-cellulose and then washed with 1% HCl solution to achieve a neutral status. The resulting α-cellulose was repeatedly washed with deionized water to ensure the sample free of reagents. The α-cellulose sample was homogenized with an ultrasonic probe and then freeze dried.

About 35-65-μg of a dried α-cellulose sample was combusted with CuO wire in a sealed quartz tube under vacuum at 900°C. The CO₂ produced was cryogenically purified off-line and introduced into an isotope ratio mass spectrometer (IRMS Finnigan-Mat Delta V) to measure the stable carbon isotope ratio. The measured carbon isotope ratio of α-cellulose was expressed as δ¹³C_{cellulose} relative to the VPDB scale. The overall precision of replicate analyses of a sample is found to be better than ±0.1‰ and the reproducibility is <0.15‰. It should be particularly noted that the human-induced rising of atmospheric CO₂ concentration since ~1850 AD has led to the decline of δ¹³C in atmosphere CO₂, resulting in the corresponding depletion of δ¹³C in the plants, i.e., so-called Suess

Effect (Keeling et al. 2005; Royles et al. 2014). It means that the plant's $\delta^{13}\text{C}$ values (including $\delta^{13}\text{C}_{\text{cellulose}}$ values) need the Suess Effect correction. Here, the needed correction was done by adapting the recalculated correction coefficients listed in the Table 2 of McCarroll and Loader (2004) and the corrected $\delta^{13}\text{C}_{\text{cellulose}}$ was expressed as CO_2 -corrected $\delta^{13}\text{C}_{\text{cellulose}}$.

3 Results

3.1 Stratigraphy and chronology

The HYP core can be stratigraphically divided into two units (Figure 2). Sediment Unit A (68-38 cm) is a grayish, well-decomposed and sedge-dominated peat layer. Sediment Unit B (38-0 cm) is a brownish, poorly-decomposed and sedge-dominated peat layer. It should be noted that Unit A and Unit B can be further divided into several sub-units based on the LOI contents. Specifically, Unit A can be further divided into two sub-units: A1 and A2. A1 has an upward increasing trend of LOI from 29.20% to 60.51%, and A2 has a constant LOI about 58.16%. Unit B can be further divided into three sub-units: B1, B2 and B3. B1 has an

upward increasing trend from 30.82% to 69.48%; B2 has a high-amplitude fluctuations (from 38% to 70%); and B3 has a constant LOI (around 37.10%).

Four sedge AMS ^{14}C dates of HYP core were given in Table 1 and the age-depth model was showed in Figure 2 with one assumption that the age of surface layer (0 cm) was 2013 AD (i.e., -63 cal. yr BP). It should be pointed out that the "post-bomb" at depth of 8 cm is actually an useful date supporting the smoothed age at the 8-cm depth.

3.2 Humification and $\delta^{13}\text{C}_{\text{cellulose}}$ records

The variations in LOI-corrected light transmission (i.e., Hc) and CO_2 -corrected $\delta^{13}\text{C}_{\text{cellulose}}$ records with depth and age can be also divided into two major units corresponding with the two major stratigraphic units (i.e., Units A, and B in Figure 2).

Unit A (68-38 cm; ~1510~1775 AD), a well-decomposed and sedge-dominated peat layer, exhibits a steep increasing trend of Hc (from ~26% to ~65%). Accompanied is a gentler increasing trend of $\delta^{13}\text{C}_{\text{cellulose}}$ (from ~-27.5‰ to ~-25.5‰) (i.e., enrichment in $\delta^{13}\text{C}_{\text{cellulose}}$). According to the linearly regressed method, we also focus on the second-order variations superimposed on the first-

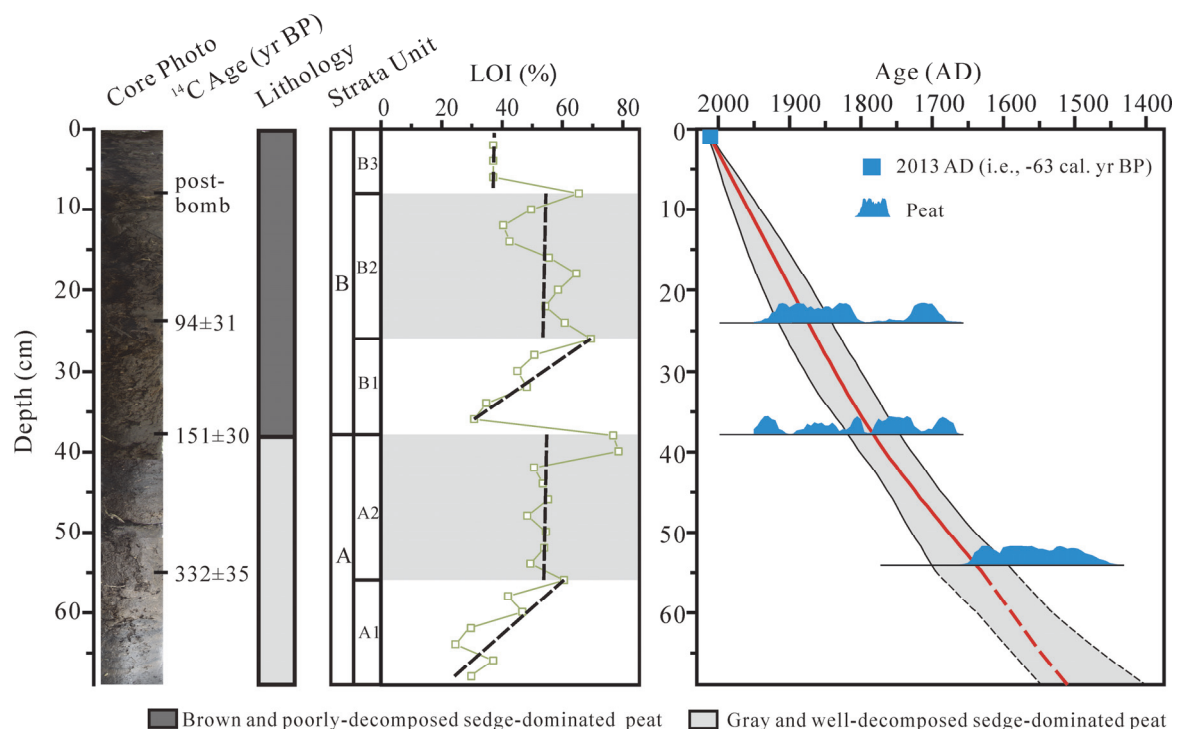


Figure 2 Peat core at Heiyangpo Peat (HYP): dates, core photo, lithology, strata units, loss on ignition (LOI) (%) and depth-age model.

order increasing trends. That is, large-amplitude second-order variations of Hc (%) are negatively related to large-amplitude second-order variations of $\delta^{13}\text{C}_{\text{cellulose}}$ (‰). For example, two major “deficit” excursions of Hc (marked with – signs in Figure 3) are correspondent with two major “enrichment” excursions of $\delta^{13}\text{C}_{\text{cellulose}}$ (marked with + signs), and a major “surplus” excursion of Hc (marked with + sign) with a major “depletion” excursion of $\delta^{13}\text{C}_{\text{cellulose}}$ (marked with – sign).

Unit B (38-0 cm; ~1775~2013 AD), a poorly-decomposed and sedge-dominated peat layer, displays a stable trend of Hc (about 40%) and an upward increasing trend of the CO₂-corrected $\delta^{13}\text{C}_{\text{cellulose}}$ values (from ~-26.8‰ to ~-24.7‰) (i.e., enrichment in $\delta^{13}\text{C}_{\text{cellulose}}$). The aforementioned second-order variations in Unit A are also observable in Unit B. For example, two “deficit” excursions and one “surplus” excursion of Hc spanning the depth of 38-10 cm are approximately correspondent with two “enrichment” excursions (marked with + signs in Figure 3) and one “depletion” excursion (marked with – sign) of CO₂-corrected $\delta^{13}\text{C}_{\text{cellulose}}$, respectively. However, an outstanding exception occurs in the topmost layer (10-0 cm: ~1950~2013 AD) where a “deficit” excursion of Hc is correspondent with a “depletion” excursion of CO₂-corrected $\delta^{13}\text{C}_{\text{cellulose}}$.

4 Reconstructions and Discussions

4.1 Reconstructions

4.1.1 Premise of used proxies

The humification was used as a peat decomposition proxy in palaeoclimatic studies (Blackford and Chambers 1993; Castro et al. 2015; Huang et al. 2013; Zhang et al. 2016). However, their palaeoclimatic implications are not straightforward. Some studies proposed that a high humification means a dry condition (Blackford and Chambers 1993; Castro et al. 2015; Chamber et al. 2011), whereas others concluded that a high humification indicates a wet condition (Huang et al. 2013; Wang et al. 2004, 2010). The former view argued that plant residues will be decayed more intensively by microbial activities in an aerobic environment during a dry condition (Blackford and Chambers, 1993; Castro et al. 2015; Chamber et al. 2011). In contrast, the latter view argued that plant residues will experience more intensive decay by microbial activities under a wet condition (Huang et al. 2013; Wang et al. 2004, 2010). The discrepancy between these two contrasting views seems to have resulted from two sources: (1) groundwater level; (2) water availability within the unsaturated layer above the groundwater level

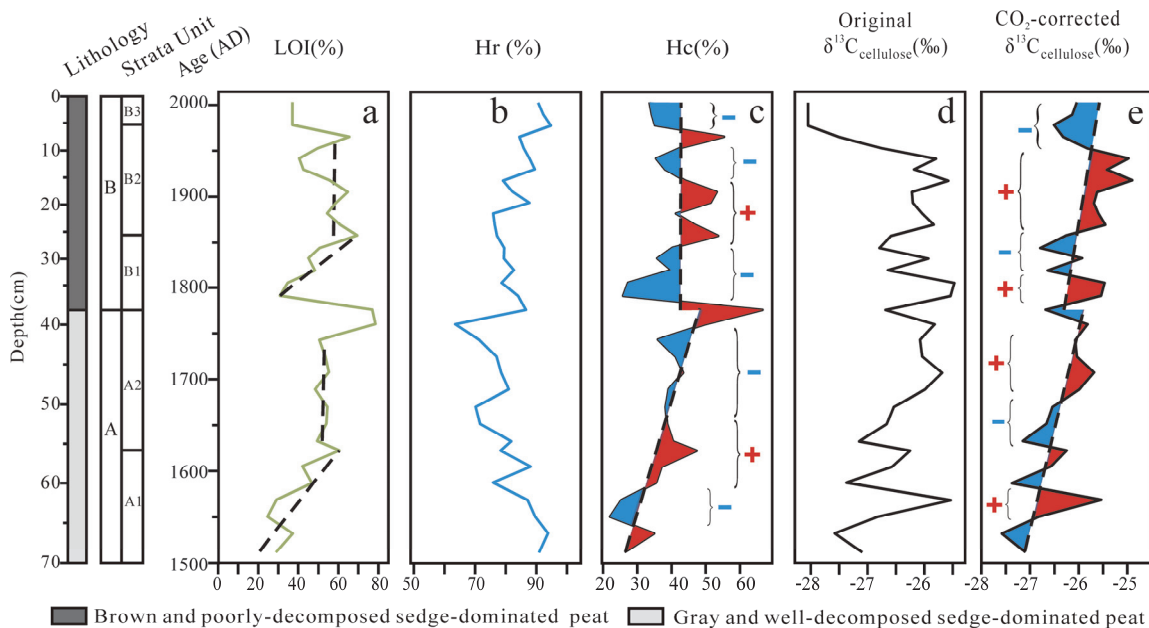


Figure 3 Variations of proxies at Heiyangpo Peat (HYP): a. loss on ignition (LOI) curve (%); b. Hr (the raw light transmission) (%); c. Hc (corrected light transmission) (%); d. original $\delta^{13}\text{C}_{\text{cellulose}}$ (‰); e. CO₂-corrected $\delta^{13}\text{C}_{\text{cellulose}}$ (corrected for the Suess Effect).

(Castro et al. 2015; Payne and Blackford 2008; Zhang et al. 2016). For example, a drop in groundwater level under a dry condition can certainly promote an aerobic environment and thus encourage peat decay within the unsaturated layer, lending a support to the former view (Chamber et al. 2011). However, if the groundwater is insignificant in supplying the plant-needed water during the growing season and also temperature is sufficiently high to stimulate microbial activities, peat decay definitely depend on the water availability within the unsaturated layer, boosting the second view (Huang et al. 2013; Wang et al. 2004).

Stable carbon isotope fractionation in peat sedges, i.e., the ratio of cellulose stable carbon isotopes ($\delta^{13}\text{C}_{\text{cellulose}}$), is primarily governed by the soil moisture level through opening or closing their leaf stomata (Menot and Burns 2001). Higher $\delta^{13}\text{C}_{\text{cellulose}}$ values (i.e., less negative) are widely reported to be associated with drier conditions and lower values (i.e., more negative) with wetter conditions (Menot and Burns 2001). A negative correlation between the $\delta^{13}\text{C}$ values in modern herbaceous plants and the land-surface moisture levels was repeatedly advocated for some Chinese peats (Hong et al. 2001, 2003, 2005) and confirmed in other cases (Lee et al. 2005; Wang et al. 2008; Ma et al. 2007, 2012; Yu 2013). Most relevant to our peat $\delta^{13}\text{C}_{\text{cellulose}}$ study at Heiyangpo Peat (HYP) in the southern Altai Mountains is a peat $\delta^{13}\text{C}_{\text{cellulose}}$ study at Chaiwopu Peat in the central Tianshan Mountains (Hong et al. 2014). The parallel climbing trends were showed between the $\delta^{13}\text{C}_{\text{cellulose}}$ -indicated moisture level at Chaiwopu Peat in the southern margin of Northern Xinjiang (Hong et al. 2014) and the pollen-indicated moisture level in entire Northern Xinjiang (Ran and Feng 2013; Ran et al. 2015; Wang and Feng 2013) during the past ~8000 years. This seems to boost our confidence on the reported negative correlation between peat $\delta^{13}\text{C}_{\text{cellulose}}$ values and land-surface moisture levels though methanogenic CH_4 as a potential limit to the interpretation of our results (Raghoebarsing et al. 2005).

4.1.2 Climatic reconstructions

One reminder needs mentioning. The growing season of peat plants in the Altai Mountains is approximately from May to September, and over 65% of the total annual precipitation occurs during

the growing season (Azien et al. 2006; Hong et al. 2014). It implicates that the variations in the peat $\delta^{13}\text{C}_{\text{cellulose}}$ values may be highly dependent on the land-surface moisture variations during the growing season. This implication appears to be supported by the HYP reality where sedge growth nearly completely relies on the growing-season water availability.

Based on the climatic indicators of used proxies ($\delta^{13}\text{C}_{\text{cellulose}}$ and humification), we can conclude that the peat decay was weakening while the growing-season soil moisture was declining during the period from ~1510 to ~1775 AD. The peat decay kept a stable level while the growing-season soil moisture was consistently declining during the period from ~1775 to 2013 AD. Superimposed on the first-order negative relationship between the Hc (%) and the $\delta^{13}\text{C}_{\text{cellulose}}$ (‰), the second-order negative relationship means that the peat decay was more effective when the growing-season soil moisture was lower on the second-order time scale during the period from ~1510 to ~1950 AD. However, an outstanding exception occurs in the topmost layer between ~1950 and ~2013 AD where a “deficit” excursion of Hc is correspondent with a “depletion” excursion of CO_2 -corrected $\delta^{13}\text{C}_{\text{cellulose}}$, suggesting that the peat decay was strong under a wet condition.

4.2 Discussions

4.2.1 Backgrounds of temperature and precipitation variations

The changes in solar irradiance (Figure 4a; Velascho Herrera et al. 2015) and also in atmospheric CO_2 concentration (Figure 4b; Macfarling et al. 2006) have driven the temperature variability of the past 1000 years (Figure 4c; Mann et al. 2009) in Northern Hemisphere. As for the precipitation in southern Siberia including the southern Altai Mountains and the Junggar Basin of northern Xinjiang, the changes in solar irradiance and in CO_2 concentration may have indirectly controlled the variability of the past 1000 years via modulating the Atlantic Multidecadal Oscillations (AMO) (Chen et al. 2013; Lan et al. 2017; Sun et al. 2015). The AMO, defined as the sea-surface temperature difference between the North Atlantic Ocean and

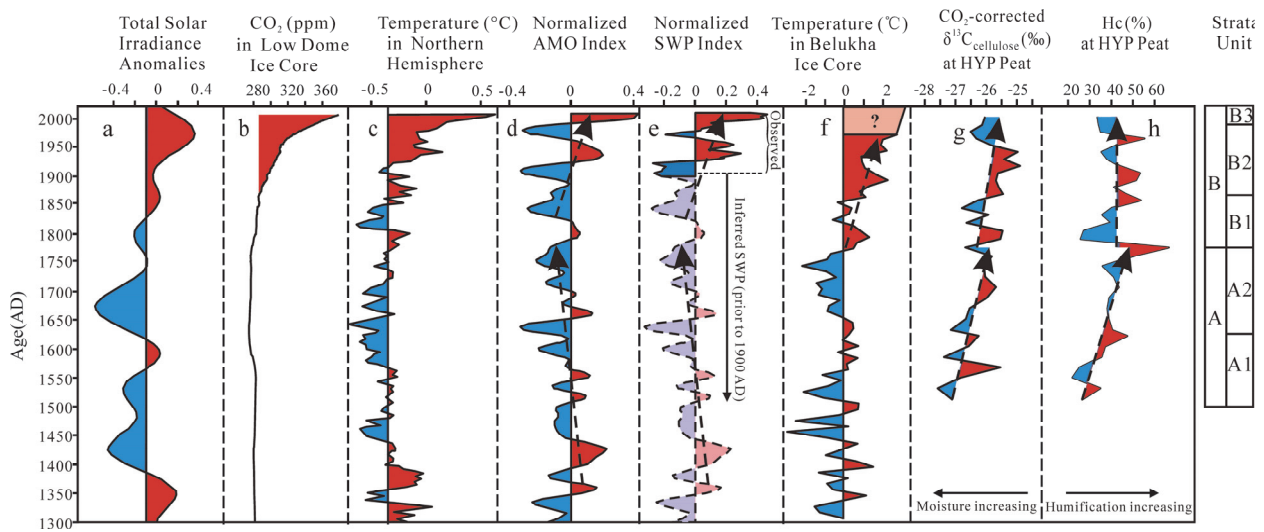


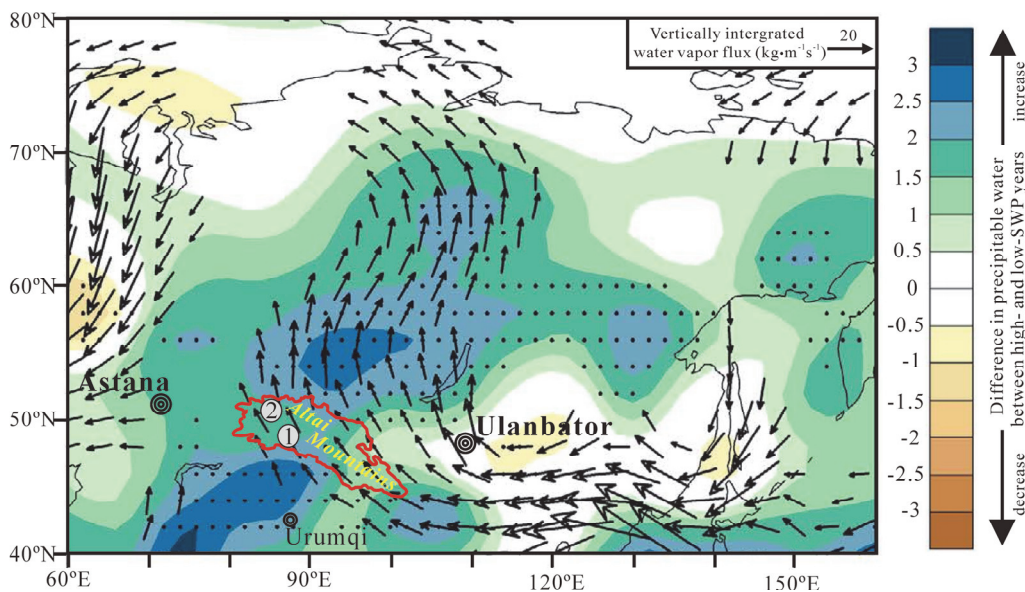
Figure 4 HYP land-surface moisture variations and the attributions: a. normalized total solar irradiance annual anomaly (W/m^2) (Velasco Herrera et al. 2015); b. CO_2 concentration (ppm) in Low Dome Ice Core (Macfarling et al. 2006); c. temperature anomaly ($^{\circ}C$) in the Northern Hemisphere (Mann et al. 2009); d. normalized AMO (i.e., Atlantic Multidecadal Oscillation) index (Wang et al. 2017); e. inferred SWP (i.e., Siberian Warm-season Precipitation) index (Sun et al. 2015; Wang et al. 2017); f. Belukha Ice Core temperature ($^{\circ}C$) in the northern Altai Mountains within Russia (Eichler et al. 2009); g. CO_2 -corrected $\delta^{13}C_{cellulose}$ variations; h, Hc (%).

the global oceans (between $60^{\circ}N$ and $45^{\circ}S$) (Mohino et al. 2011), is reported to be one of the most important climatic forcing factors on decadal/multi-decadal scales affecting southern Siberia (Lu et al. 2006).

Situated in the westerly's influencing zone, southern Siberia is documented to have been strongly influenced by AMO (Chen et al. 2013; Lan et al. 2017; Sun et al. 2015). Specifically, a robust positive relationship ($r^2=0.72$) between the normalized AMO index and the normalized SWP index (SWP: Siberian warm-season precipitation) was observed between 1901 and 2013 AD (i.e., topmost portion of Figure 4e). The mechanistic linkage between AMO and SWP was illustrated using re-analysis data and simulation techniques. As shown in Figure 5 (modified from Figure 3c in Sun et al. 2015), the composite differences in vertically integrated (1000-400 hPa) water-vapor flux anomaly and in the precipitable water anomaly between high and low warm-season precipitation years are extremely significant and the significance was mechanistically attributable to the teleconnection pattern excited by positively-phased AMO. That is, an east-west dipole structure covering the Eurasian continent leads to intensification of the transport of vertically integrated water vapor flux mainly from northern

Pacific Ocean during positive AMO phases, favoring the increase of precipitable water flux in southern Siberia (Sun et al. 2015).

If the mechanistically-linked positive relationship ($r^2=0.72$) between the normalized AMO index and the normalized SWP index for the period from 1901 to 2013 AD also holds for the past millennium, the normalized SWP index of the past millennium can be approximated based on the normalized AMO index, meaning that the extrapolated normalized SWP index curve (Figure 4e) can be taken as a warm-season precipitation curve of the past millennium in southern Siberia (see Figure 5). This view is supported by the in-phase relationship between the reconstructed AMO index (Gray et al. 2004) and tree-ring-based precipitation and stream flow reconstructions in the southern Altai in the past two hundred years (Chen et al. 2016a, b). In terms of temperature of the past millennium, the most reliable and also the most relevant is an ice-core $\delta^{18}O$ -based reconstruction from the Belukha Glacier in the northern Altai Mountains (see Figure 1 and Figure 5 for the ice-core location). A strong correlation ($r^2=0.69$) between the $\delta^{18}O$ values of the Belukha ice core and the instrument-recorded March-November temperatures of the past century at a nearby meteorological station suggests that $\delta^{18}O$ -



① Heiyangpo peat core ② Belukha Ice Core sampling site

Figure 5 Composite differences of high-SWP (Siberian Warm-season Precipitation) years minus low-SWP years in vertically integrated moisture flux (vectors; $\text{kg m}^{-1} \text{s}^{-1}$) and precipitable water fields (shading) over northern Asia (modified from Sun et al. 2015). Note: the length and direction of arrows mean the flux and transported direction of vertically integrated water vapor.

based temperature curve of the past ~750 years (Eichler et al. 2009) is a highly acceptable warm-season temperature curve (Figure 4f).

4.2.2 Interpretation of moisture variations in the southern Altai Mountains

The widely-reported negative correlation between peat $\delta^{13}\text{C}_{\text{cellulose}}$ values and land-surface moisture levels is the basis for deciphering the peat $\delta^{13}\text{C}_{\text{cellulose}}$ variations of HYP Peat. The warm-season precipitation variations inferred from the AMO reconstruction (Figure 4e; Wang et al. 2017; Sun et al. 2015) and the warm-season temperature variations reconstructed from the Belukha ice core (Figure 4f; Eichler et al. 2009) are the references for interpreting the moisture variations of the past 500 years at HYP Peat. As shown in Figure 4g, the peat $\delta^{13}\text{C}_{\text{cellulose}}$ -suggested moisture level has been generally declining during the past 500 years at HYP Peat. The general declining trend from ~1510 to ~1775 AD may be attributable to the declining trend of the inferred Siberian warm-season precipitation (i.e., inferred SWP index in Figure 4e) under low-temperature conditions (Figure 4f). The general declining trend from ~1775 to ~2013 AD may be attributable to the increasing trend of

warm-season temperature (Figure 4f) under increasing-precipitation conditions (Figure 4e).

Our attention now turns to the Hc (i.e., humification) to more fully understand the hydrologic variations of HYP Peat (Figure 4h). The first-order parallel increasing trends between the Hc values (i.e., humification decreasing; see Figure 4h) and the $\delta^{13}\text{C}_{\text{cellulose}}$ values (i.e., moisture decreasing; see Figure 4g) within the depths spanning from 68 cm to 38 cm suggest that peat decay was weakening when the land-surface moisture level was declining during the period from ~1510 to ~1775 AD. It implies that a constant drying condition may have inhibited peat decay within the unsaturated layer above the groundwater level (Chamber et al. 2011). The cause for the moisture-level dropping was most likely a constant decline of precipitation, especially warm-season (i.e., growing-season) precipitation (see Figure 4e). And, the low temperature-resulted decrease in evaporation might not be sufficient to counteract the decreasing precipitation-resulted decline in land-surface moisture. The first-order different trends between the stable Hc values and the increasing $\delta^{13}\text{C}$ values (i.e., moisture decreasing) within the depths spanning from 38 cm to 0 cm suggest that the peat humification could be

explained by the steady decomposition of peat in the acrotelm when the land-surface moisture level was declining during the period from ~1775 to ~2013 AD. It implies that peat decay did not depend on the water availability (or land-surface moisture level) within the unsaturated layer above the groundwater level or depend on an aerobic environment in the acrotelm. It also means that the groundwater was insignificant in supplying the plant-needed water (Huang et al. 2013). The cause for the land-surface moisture-level dropping was most likely a constant rise of the warm-season temperature (see Figure 4f). And, the AMO-suggested increase in precipitation might not be sufficient to counteract the rising temperature-resulted decline in land-surface moisture.

Our attention is now devoted to the second-order variations of Hc (%) and $\delta^{13}\text{C}_{\text{cellulose}}$ (‰) that are superimposed on the first-order variations. That is, large-amplitude second-order variations of Hc are negatively related to large-amplitude second-order variations of the $\delta^{13}\text{C}_{\text{cellulose}}$ (see Figure 3). For example, those major “surplus” (“deficit”) excursions of Hc correspond with those major “depletion” (“enrichment”) excursions of $\delta^{13}\text{C}_{\text{cellulose}}$, suggesting that the peat decay was more (less) effective when the growing-season land-surface moisture level was lower (higher) on the second-order time scale. It implies that peat decay depended on an aerobic environment within the unsaturated layer above the groundwater level on the second-order time scale. Admittedly, we do not have sufficient data at this stage of research to attribute the second-order negative relationships from ~1510 and ~1950 AD to the changes in precipitation or/and in temperature. But, the second-order positive relationship between Hc (a “deficit” excursion) and $\delta^{13}\text{C}_{\text{cellulose}}$ (also a “depletion” excursion) in the topmost layer (10-0 cm) covering the period from ~1950 to ~2013 AD (see Figure 3) may be attributable to the observed dramatic increase in the precipitation and high temperature since ~1950 AD in northern Xinjiang and the adjacent areas (Chen et al. 2012; Xu et al. 2010, 2015). It implies that peat decay might

depend on high-temperature-stimulated active microbial activities under the increasing-precipitation conditions.

5 Conclusions

(1) The humification increasing trend and the $\delta^{13}\text{C}_{\text{cellulose}}$ -suggested moisture decreasing trend within the depths spanning from 68 cm to 38 cm implies that a constant drying condition may have inhibited peat decay from ~1510 to ~1775 AD. The moisture-level dropping was most likely resulted from a constant decline of the precipitation.

(2) The humification kept a stable trend and the $\delta^{13}\text{C}_{\text{cellulose}}$ -suggested moisture decreasing trend within the depths spanning from 38 cm to 0 cm implies that peat decay did not depend on the water availability (or land-surface moisture level) or depend on an aerobic environment in the acrotelm from ~1775 to ~2013 AD. The land-surface moisture-level dropping was most likely resulted from a constant rise of the warm-season temperature.

(3) Although we do not have sufficient data to attribute the second-order negative relationships between the humification and the $\delta^{13}\text{C}_{\text{cellulose}}$ from ~1510 to ~1950 AD and the changes in precipitation or/and in temperature, the second-order positive relationship from ~1950 to ~2013 AD may be attributable to high-temperature-stimulated active microbial activities under the high precipitation conditions.

Acknowledgement

This research was financially supported by Chinese Natural Science International Cooperation Program Foundation Grant (No. 41361140361), Chinese Natural Science Foundation Grant (No. U1203821Lo8) and Chinese Academy Sciences International Cooperation Program (No. GJHZ201315). We thank Prof. Nurbayev Abdusalih for his help in identifying plant residues.

References

Aaby B, Tauber H (1975) Rates of peat formation in relation to degree of humification and local environment, as shown by

studies of a raised bog in Denmark. *Boreas* 4: 1-17. <https://doi.org/10.1111/j.1502-3885.1975.tb00675.x>

- Aizen VB, Aizen EM, Joswiak DR, et al. (2006) Climatic and atmospheric circulation pattern variability from ice-core isotope/ geochemistry records (Altai, Tian Shan and Tibet). *Annals of Glaciology* 43(1): 49-60. <https://doi.org/10.3189/172756406781812078>
- Batima P, Natsagdorj L, Gombluudev P, et al. (2005) Observed climate change in mongolia, assessments of impacts and adaptations to climate change working paper, 26
- Blackford J, Chambers F (1993) Determining the degree of peat decomposition for peat-based palaeoclimatic studies. *International Peat Journal* 5: 7-24
- Blaauw M (2010) Methods and code for 'classical' age-modelling of radiocarbon sequences. *Quaternary Geochronology* 5: 512-5128. <https://doi.org/10.1016/j.quageo.2010.01.002>
- Castro D, Souto M, Garcia-Rodeja E, et al. (2015) Climate change records between the mid- and late Holocene in a peat bog from Serra do Xistral (SW Europe) using plant macrofossils and peat humification analyses. *Palaeogeography Palaeoclimatology Palaeoecology* 420: 82-95. <https://dx.doi.org/10.1016/j.palaeo.2014.12.005>
- Chambers FM, Beilman DW, Yu Z, (2011) Methods for determining peat humification and for quantifying peat bulk density, organic matter and carbon content for palaeostudies of climate and peatland carbon dynamics. *Mires Peat* 7: 1-10. <http://www.mires-and-peat.net/> Available on: <http://mires-and-peat.net/pages/volumes/map07/map0707.php>
- Chen F, Yuan YJ, Chen FH, et al. (2013) A 426-year drought history for Western Tian Shan, Central Asia, inferred from tree rings and linkages to the North Atlantic and Indo-Pacific oceans. *Holocene* 23: 1095-1104. <https://doi.org/10.1177/0959683613483614>
- Chen F, Yuan Y, Zhang T, et al. (2016a) Precipitation reconstruction for the northwestern Chinese Altay since 1760 indicates the drought signals of the northern part of inner Asia. *International Journal of Biometeorology* 60(3): 455-463. <https://doi.org/10.1007/s00484-015-1043-5>
- Chen F, Yuan Y, Davi N, et al. (2016b) Upper Irtysh River flow since AD 1500 as reconstructed by tree rings, reveals the hydroclimatic signal of inner Asia. *Climatic Change* 139(3-4): 651-665. <https://doi.org/10.1007/s10584-016-1814-y>
- Chen X (2010) *Physical Geography of China's Arid Zones*, Science Press, Beijing. (in Chinese)
- Chen YN, Yang Q, Luo Y, et al. (2012) Ponder on the issues of water resources in the arid region of northwest China. *Arid Land Geography* 35(1): 1-9. (in Chinese) <https://doi.org/10.13826/j.cnki.cn65-1103/x.2012.01.007>
- Eichler A, Oliver S, Henderson K, et al. (2009) Temperature response in the Altai region lags solar forcing. *Geophysics Research Letters* 36: L01808. <https://doi.org/10.1029/2008GL035930>
- Fei J, Wu ZH, Huang JP, et al. (2014) Evolution of land surface air temperature trend. *Nature Climate Change* 4(6): 462. <https://doi.org/10.1038/NCLIMATE2223>
- Gray ST, Graumlich LJ, Betancourt JL, et al. (2004) A tree-ring based reconstruction of the Atlantic Multidecadal Oscillation since 1567 AD. *Geophysical Research Letters* 31: L12205. <https://doi.org/10.1029/2004GL019932>
- Green JW (1963) Wood cellulose. In Whistler, R.L., editor, *Methods in carbohydrate chemistry*, vol. 3, Academic Press, New York.
- Hong B, Gasse F, Uchida M, et al. (2014) Increasing summer rainfall in arid eastern-Central Asia over the past 8500 years. *Scientific Reports* 4: 5279. <https://doi.org/10.1038/srepo5279>
- Hong YT, Hong B, Lin QH, et al. (2003) Correlation between Indian Ocean summer monsoon and North Atlantic climate during the Holocene. *Earth and Planetary Science Letters* 211: 371-380. [https://doi.org/10.1016/S0012-821X\(03\)00207-3](https://doi.org/10.1016/S0012-821X(03)00207-3)
- Hong YT, Hong B, Lin QH, et al. (2005) Inverse phase oscillations between the East Asian and Indian Ocean summer monsoons during the last 12000 years and paleo-El Niño. *Earth Planetary Science Letters* 231: 337-346. <https://doi.org/10.1016/j.epsl.2004.12.025>
- Hong YT, Wang ZG, Jiang HB, et al. (2001) A 6000-year record of changes in drought and precipitation in northeastern China based on a $\delta^{13}\text{C}$ time series from peat cellulose. *Earth Planetary Science Letters* 185: 111-119. [https://doi.org/10.1016/S0012-821X\(00\)00367-8](https://doi.org/10.1016/S0012-821X(00)00367-8)
- Huang C, Li YH, Guo WK, et al. (2015) The experimental methods of extraction α -cellulose in peat samples. *Arid Land Geography* 38(4): 728-734. (In Chinese)
- Huang JP, Yu HP, Guan XD, et al. (2015) Accelerated dryland expansion under climate change. *Nature Climate Change* 6: 166-171. <https://doi.org/10.1038/NCLIMATE2837>
- Huang T, Cheng SG, Mao XM, et al. (2013) Humification degree of peat and its implications for Holocene climate change in Hani peatland, Northeast China. *Chinese Journal of Geochemistry* 32 (4): 406-412. <https://doi.org/10.1007/s11631-013-0649-8>
- Keeling CD, Piper SC, Bacastow RB, et al. (2005) Atmospheric CO_2 and ^{13}C exchange with the terrestrial biosphere and oceans from 1978 to 2000: Observations and carbon cycle implications. In: Ehleringer JR, Cerling TE and Dearing MD (eds) *A History of Atmospheric CO_2 and Its Effects on Plants, Animals, and Ecosystems*. Springer Verlag, New York, 83-113.
- Kutzbach JE, Chen G, Cheng H, et al. (2014) Potential role of winter rainfall in explaining increased moisture in the Mediterranean and Middle East during periods of maximum orbitally-forced insolation seasonality. *Climate Dynamics* 42(3-4): 1079-1095. <https://doi.org/10.1007/s00382-013-1692-1>
- IPCC (2014) In: Stocker, T.F., Qin, D.H., Plattner, G.K., Tignor, M., Allen, S.K., Boschung, J., Nauels, A., Xia, Y., Bex, V., Midgley, P.M. (Eds.), *Climate Change 2013: the Physical Science Basis*. Working Group I Contribution to the Fifth Assessment Report of the Intergovernmental Panel on Climate Change. Cambridge University Press, Cambridge, United Kingdom and New York, NY, USA
- Lan B, Zhang DL, Yang YP (2017) Evolution of Lake Ailike (northern Xinjiang of China) during past 130 years inferred from diatom data. *Quaternary International*. <https://doi.org/10.1016/j.quaint.2016.11.014>
- Lee X, Feng Z, Guo L, et al. (2005) Carbon isotope of bulk organic matter, a proxy for precipitation in the arid and semiarid central East Asia. *Global Biogeochemical Cycles* 19: GB4010. <https://doi.org/10.1029/2004GB002303>
- Lu R, Dong B, Ding H (2006) Impact of the Atlantic Multidecadal Oscillation on the Asian summer monsoon. *Geophysical Research Letters* 33: L24701. <https://doi.org/10.1029/2006GL027655>
- Ma JY, Sun W, Liu XN, et al. (2012) Variation in the Stable Carbon and Nitrogen Isotope Composition of Plants and Soil along a Precipitation Gradient in Northern China. *PLoS ONE* 7(12): e51894. <https://doi.org/10.1371/journal.pone.0051894>
- Ma JY, Chen FH, Zhang HW, et al. (2007) Spatial distribution characteristics of stable carbon isotope compositions in desert plant *Reaumuria soongorica*. *Frontier Earth Science China* 1(2): 150-156. <https://doi.org/10.1007/s11707-007-0019-0>
- MacFarling MC, Etheridge D, Trudinger C, et al. (2006) Law Dome CO_2 , CH_4 and N_2O ice core records extended to 2000 years BP. *Geophysical Research Letters* 33: L14810. <https://doi.org/10.1029/2006GL026152>
- Mann ME, Zhang Z, Rutherford S, et al. (2009) Global signatures and dynamical origins of the Little Ice Age and Medieval Climate Anomaly. *Science* 326: 1256-1260. <https://doi.org/10.1126/science.1177303>
- Mariotti A (2007) How ENSO impacts precipitation in southwest central Asia. *Geophysical Research Letters* 34(16): L16706. <https://doi.org/10.1029/2007GL030078>
- McCarroll D, Loader NJ (2004) Stable isotopes in tree rings. *Quaternary Science Reviews* 23: 771-801. <https://doi.org/10.1016/j.quascirev.2003.06.017>
- Ménot G, Burns SJ (2001) Carbon isotopes in ombrogenic peat

- bog plants as climatic indicators, calibration from an altitudinal transect in Switzerland. *Organic Geochemistry* 32: 233-245. [https://doi.org/10.1016/S0146-6380\(00\)00170-4](https://doi.org/10.1016/S0146-6380(00)00170-4)
- Mohino E, Janicot S, Bader J (2011) Sahel rainfall and decadal to multi-decadal sea surface temperature variability. *Climate dynamics* 37: 419-440. <https://doi.org/10.1007/s00382-010-0867-2>
- Nurbayev A, Niels T, Altaï A, et al. (2008) Peatlands of the Chinese Altay. *Peatlands International* 2: 25-28.
- Payne R, Blackford J (2008) Peat humification and climate change: a multi-site comparison from mires in south-east Alaska. *Mires Peat* 3: 1-11
- R development core team (2013) *RA Lang Environ Stat Comput* 55: 275-286
- Raghoebarsing AA, Smolders AJP, Schmid MC, et al. (2005) Methanotrophic symbionts provide carbon for photosynthesis in peat bogs. *Nature* 436(7054): 1153. <https://doi.org/10.1038/nature03802>
- Ran M, Feng ZD (2013) Holocene moisture variations across China and driving mechanisms: a synthesis of climatic records. *Quaternary International* 313/314: 179-193. <https://doi.org/10.1016/j.quaint.2013.09.034>
- Ran M, Zhang CJ, Feng ZD (2015) Climatic and hydrological variations during the past 8000 years in northern Xinjiang of China and the associated mechanisms. *Quaternary International* 358: 21-34. <https://doi.org/10.1016/j.quaint.2014.07.056>
- Reimer PJ, Bard E, Bayliss A, et al. (2013) IntCal13 and Marine13 radiocarbon age calibration curves, 0–50,000 years cal BP. *Radiocarbon* 55: 1869-1887. https://doi.org/10.2458/azu_js_rc.55.16947
- Royles J, Horwath AB, Griffiths H (2014) Interpreting bryophyte stable carbon isotope composition: plants as temporal and spatial climate recorders. *Geochemistry, Geophysics, Geosystems* 15:1462-1475. <https://doi.org/10.1002/2013GC005169>
- Salnikov V, Turulina G, Polyakova S, et al. (2015) Climate change in Kazakhstan during the past 70 years. *Quaternary International* 358: 77-82. <https://doi.org/10.1016/j.quaint.2014.09.008>
- Sorg A, Bolch T, Stoffel M, et al. (2012) Climate change impacts on glaciers and runoff in Tien Shan (Central Asia). *Nature Climate Change* 2: 725-731. <https://doi.org/10.1038/NCLIMATE1592>
- Sun C, Li J, Zhao S (2015) Remote influence of Atlantic multidecadal variability on Siberian warm season precipitation. *Scientific Reports* 5: 16853. <http://doi.org/10.1038/srep16853>
- Velasco Herrera VM, Mendoza B, Herrera GV (2015) Reconstruction and prediction of the total solar irradiance: From the Medieval Warm Period to the 21st century. *New Astronomy* 34: 221-233. <https://doi.org/10.1016/j.newast.2014.07.009>
- Wang J, Yang B, Ljungqvist FC, et al. (2017) Internal and external forcing of multidecadal Atlantic climate variability over the past 1,200 years. *Nature Geoscience* 10(7): 512-517. <https://doi.org/10.1038/NGEO2962>
- Wang H, Hong YT, Zhu YX, et al. (2004) Humification degrees of peat in Qinghai-Xizang Plateau and palaeoclimate change. *Chinese Science Bulletin* 5: 514-519. <https://doi.org/10.1360/03wd0584>
- Wang H, Hong YT, Lin QH, et al. (2010) Response of humification degree to monsoon climate during the Holocene from the Hongyuan peat bog, eastern Tibetan Plateau. *Palaeogeography Palaeoclimatology Palaeoecology* 3: 171-177. <https://doi.org/10.1016/j.palaeo.2009.12.015>
- Wang G, Feng X, Han J, et al. (2008) Paleovegetation reconstruction using $\delta^{13}C$ of soil organic matter. *Biogeosciences* 5: 1325-1337. Available on: <https://hal.archives-ouvertes.fr/hal-00298000/document>
- Wang W, Feng ZD (2013) Holocene moisture evolution across the Mongolian Plateau and its surrounding areas: A synthesis of climatic records. *Earth-Science Reviews* 122: 38-57. <https://doi.org/10.1016/j.earscirev.2013.03.005>
- Wei X, Chen JY (2012) The climatic characters of precipitation in Northern Xinjiang and its response to ENSO. *Progress in geophysics* 12:753-759. (in Chinese)
- Xu CC, Chen YN, Yang YH, et al. (2010) Hydrology and water resources variation and its response to regional climate change in Xinjiang. *Journal of Geographical Sciences* 20(4): 599-612. <https://doi.org/10.1007/s11442-010-0599-6>
- Xu CC, Li JX, Zhao J, et al. (2015) Climate variations in northern Xinjiang of China over the past 50 years under global warming. *Quaternary International* 358: 83-92. <https://doi.org/10.1016/j.quaint.2014.10.025>
- Yu SY (2013) Quantitative reconstruction of mid- to late-Holocene climate in NE China from peat cellulose stable oxygen and carbon isotope records and mechanistic models. *The Holocene* 23(11): 1507-1516. <https://doi.org/10.1177/0959683611425544>
- Zhang Y, Meyers PA, Liu XY, et al. (2016) Holocene climate changes in the central Asia mountain region inferred from a peat sequence from the Altai Mountains, Xinjiang, northwestern China. *Quaternary Science Reviews* 152: 19-30. <https://doi.org/10.1016/j.quascirev.2016.09.016>